ISSN(Online) : 2319 - 8753
ISSN (Print) : 2347 - 6710

International Journal of Innovative Research in Science, Engineering and Technology

(An ISO 3297: 2007 Certified Organization)

Vol. 4, Special Issue 6, May 2015

Simplified Reactive Power Control for Single-Phase Grid-Connected Photovoltaic Inverters

[1]Dr.C.Nagarajan,[2]G. Neelakrishnan, [3]V.Sundarajan, [3]D.Vinoth

[1]Professor, Department of EEE, Muthayammal College of Engineering, Rasipuram, Tamilnadu, India

[2]Assistant Professor, Department of EEE, Muthayammal College of Engineering, Rasipuram, Tamilnadu, India

[3]PG Scholar, Department of EEE, Muthayammal College of Engineering, Rasipuram, Tamilnadu, India

ABSTRACT: A simple photovoltaic (PV) system capable of operating in grid-connected mode and using multilevel boost converter (MBC) and line commutated inverter (LCI) has been developed for extracting the maximum power and feeding it to a single phase utility grid with harmonic reduction. Theoretical analysis of the proposed system is done and the duty ratio of the MBC is estimated for extracting maximum power from PV array. For a fixed firing angle of LCI, the proposed system is able to track the maximum power with the determined duty ratio which remains the same for all irradiations. This is the major advantage of the proposed system which eliminates the use of a separate maximum power point tracking (MPPT) Experiments have been conducted for feeding a single phase voltage to the grid. So by proper and simplified technique we are reducing the harmonics in the grid for unbalanced loads.

I. INTRODUCTION

The increasing demand for energy, the continuous reduction in existing sources of fossil fuels and the growing concern regarding environment pollution, have pushed mankind to explore new technologies for the production of electrical energy using clean, renewable sources, such as solar energy, wind energy, etc. Among the non-conventional, renewable energy sources, solar energy affords great potential for conversion into electric power, able to ensure an important part of the electrical energy needs of the planet. The conversion of solar light into electrical energy represents one of the most promising and challenging energetic technologies, in continuous development, being clean, silent and reliable, with very low maintenance costs and minimal ecological impact. Solar energy is free, practically inexhaustible, and involves no polluting residues or greenhouse gases emissions.

II. PHOTO VOLTAICS

The electrical potential developed between two dissimilar materials when their common junction is illuminated with radiation of photon. The photovoltaic cell, thus, converts light directly into electricity. The pv effect was discovered in 1839 by French physicist Becquerel.

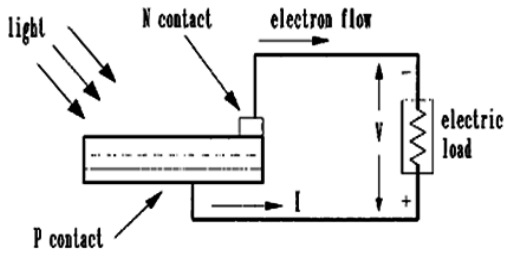

Fig.1.The Photo Voltaic Effect

ISSN(Online) : 2319 - 8753
ISSN (Print) : 2347 - 6710

International Journal of Innovative Research in Science, Engineering and Technology

(An ISO 3297: 2007 Certified Organization)

Vol. 4, Special Issue 6, May 2015

The physics of the pv cell is very similar to the classical p-n junction diode. When light is absorbed by the junction, the energy of the absorbed photons is transferred to the electron system of the material, resulting in the creation of charge carriers that are separated at the junction. The charge carriers may be electron-ion pairs in a liquid electrolyte, or electronhole pairs in a solid semiconducting material. The charge carriers in the junction region create a potential gradient, get accelerated under the electric field and circulate as the current through an external circuit.

The origin of the photovoltaic potential is the difference in the chemical potential, called the fermi level, of the electrons in the two isolated materials. When they are joined, the junction approaches a new thermodynamic equilibrium. Such equilibrium can be achieved only when the Fermi level is equal in the two materials. This occurs by the flow of electrons from one materialto the other until a voltage difference is established between the two materials which have the potential just equal to the initial difference of the Fermi level. This potential drives the photocurrent.

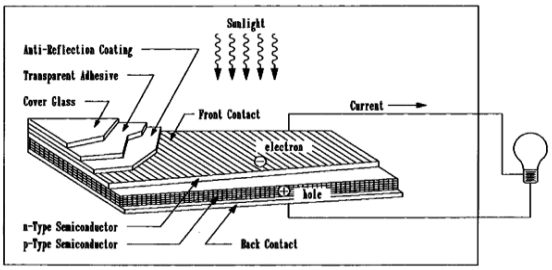

Fig.2.Construction of PV cell

III. MODULE AND ARRAY

The solar cell described above is the basic building block of the pv power system. Typically, it is a few square inches in size and produces about one watt of power. For obtaining high power, numerous such cells are connected in series and parallel circuits on a panel (module) area of several square feet. The solar array or panel is defined as a group of several modules electrically connected in series-parallel combinations to generate the required current and voltage.

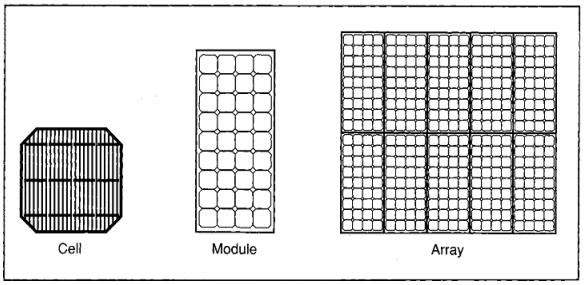

Fig.3.Cell, Module and Array

IV. EQUIVALENT CIRCUIT OF PV CELL

The complex physics of the pv cell can be represented by the equivalent electrical circuit shown. The circuit parameters are as follows.

The output-terminal current I is equal to the light-generated current IL , less the diode-current Id and the shunt-leakage current Ish. The series resistance Rs represents the internal resistance to the current flow, and depends on the p-n junction depth, the impurities and the contact resistance. The shunt resistance Rsh is inversely related with leakage current to the ground. In an ideal pv cell, Rs = 0 (no series loss), and Rsh = ∞ (no leakage to ground). In the equivalent circuit, the current delivered to the external load equals the current IL generated by the illumination, less the diode current Id and the ground-shunt current Ish. The open circuit voltage Voc of the cell is obtained when the load current is zero.

ISSN(Online) : 2319 - 8753
ISSN (Print) : 2347 - 6710

International Journal of Innovative Research in Science, Engineering and Technology

(An ISO 3297: 2007 Certified Organization)

Vol. 4, Special Issue 6, May 2015

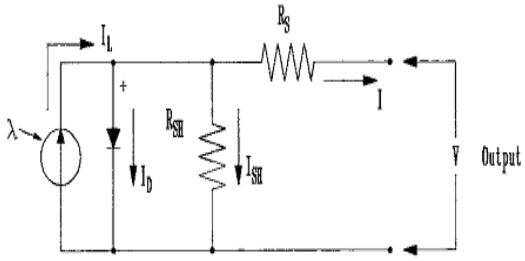

Fig.4.Equivalent Circuit of PV cell

The major factors influencing the electrical design of the solar array are as follows:

- The sun intensity.
- The sun angle.
- The load matching for maximum power.
- The operating temperature.

V. I-V AND P-V CURVES

The electrical characteristic of the pv cell is generally represented by the current versus voltage (i-v) curve.

Figure shows the i-v characteristic of a pv module under two conditions, in sunlight and in dark. In the first quadrant, the top left of the i-v curve at zero voltage is called the shortcircuit current. This is the current we would measure with the output terminals shorted (zero voltage). The bottom right of the curve at zero current is called the open-circuit voltage. This is the voltage we would measure with the output terminals open (zero current). In the left shaded region, the cell works like a constant current source, generating voltage to match with the load resistance. In the shaded region on the right, the current drops rapidly with a small rise in voltage. In this region, the cell works like a constant voltage source with an internal resistance. Somewhere in the middle of the two shaded regions, the curve has a knee point.

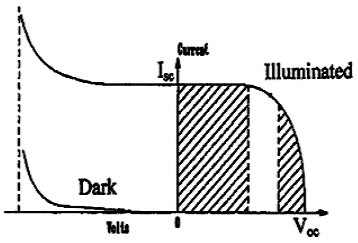

Fig.5.i-v Curve

The power output of the panel is the product of the voltage and the current outputs.

ISSN(Online) : 2319 - 8753
ISSN (Print) : 2347 - 6710

International Journal of Innovative Research in Science, Engineering and Technology

(An ISO 3297: 2007 Certified Organization)

Vol. 4, Special Issue 6, May 2015

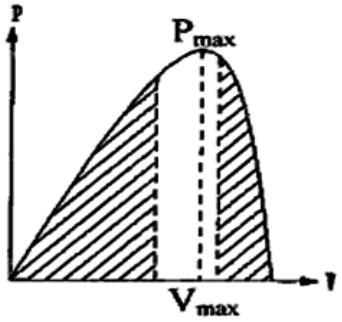

Fig.6.P-V Curve

The cell produces no power at zero voltage or zero current, and produces the maximum power at voltage corresponding to the knee point of the i-v curve. This is why pv power circuits are designed such that the modules operate closed to the knee point, slightly on the left hand side. The pv modules are modeled approximately as a constant current source in the electrical analysis of the system.

In this project the pv- cell is modelled as constant voltage source. The pv cell is modelled using following formulae.

$Vpv=-Vt*\log(Ipv/Io+1)$

$Vpv= Ipv[Vd/Rp+Io(\exp(Vd/Vt)-1)]$

$Ppv= VpvIpv$

Where,

Vpv	=	Voltage generated by PV cell.
Ipv	=	Current output of the PV cell.
Io	=	Short circuit Current.
Vt	=	Open Circuit Voltage.
Vd	=	Voltage across the diode.

VI. BOOST CONVERTERS

A boost converter topology is obtained by rearranging the components of a buck converter according to figure. During the time the switch is closed energy is transferred to the inductor while the diode is preventing the capacitor to discharge through the switch. When the switch opens current through the inductor continues to flow in the same direction as during the previous cycle. This forward-biases the diode and both the input voltage source and the inductor are transferring energy to the load. Hence, a voltage boost occurs across the load, which causes the output voltage to be higher than the input voltage. The capacitor must be large enough to keep the output voltage approximately constant

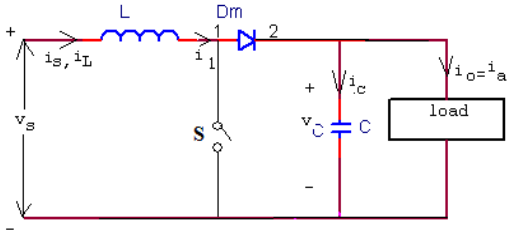

Fig.7.Boost topology.

Mode 1:

In this mode when MOSFET $M_1$is switched on at t=0.The input current, which rises, flows through inductor L and MOSFET M_1. Is this mode diagram shown in figure

ISSN(Online) : 2319 - 8753
ISSN (Print) : 2347 - 6710

International Journal of Innovative Research in Science, Engineering and Technology

(An ISO 3297: 2007 Certified Organization)

Vol. 4, Special Issue 6, May 2015

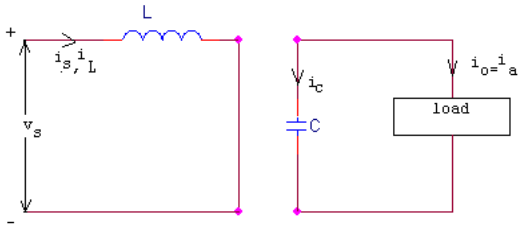

Fig.8 mode 1 operation of Boost converter

Mode 2:

In this mode when MOSFET M_1 is switched off at $t=t_1$.The current which was flowing through the MOSFET would not flow through L, C, load and diode D_m. The inductor current falls until MOSFET M_1 is turned on again in the next cycle. Is this mode diagram shown in figure

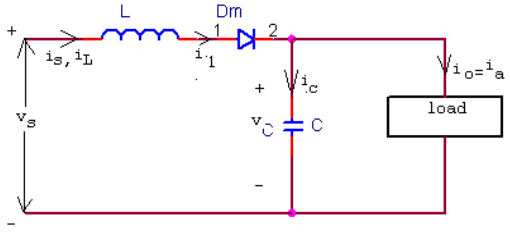

Fig.9.mode 2 operation of Boost converter

VII. HYSTERSIS CONTROL

Basic self oscillating controllers based on hysteresis are well described in the literature. The hysteresis controller can be made with either a current- or a voltage loop. The benefits of hysteresis controllers are primarily the linear modulation caused by the saw tooth-shaped carrier with ideally straight slopes, and by the infinite power supply rejection ratio, PSRR, if the supply variation can be considered very slow compared to the switching frequency. Power supply variations at higher frequencies are not suppressed totally, and will result in sum and difference products of the reference signal and the power supply variation, but these still meets high suppression. For use in audio amplifier applications, the hysteresis controller is very desirable due to the high linearity and simple design. However, hysteresis controllers suffers from a switching frequency dependent on the modulation index, M, of the amplifier. All other basic types of self oscillating modulators suffer from this phenomenon too.

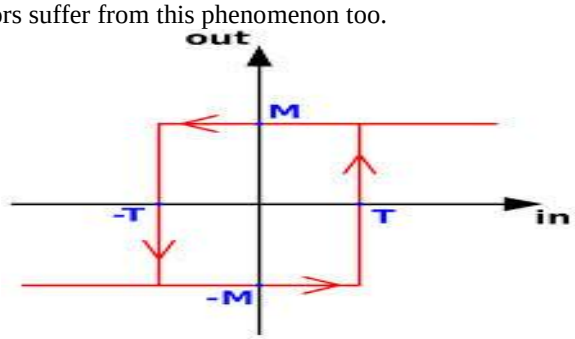

Fig.10.Frequency ripple voltage

VIII. HYSTERSIS CONTROLLER

If the variable hysteresis window is made such that it follows the square of the absolute value as well as the derivative of the input signal, the switching frequency can be made constant, but at a much higher system complexity than the basic design. In this paper a second integrator block inserted before the hysteresis window in either a current or a

ISSN(Online) : 2319 - 8753
ISSN (Print) : 2347 - 6710

International Journal of Innovative Research in Science, Engineering and Technology

(An ISO 3297: 2007 Certified Organization)

Vol. 4, Special Issue 6, May 2015

voltage mode controller is proposed to obtain a close to constant switching frequency, regardless of M. The extra integrator integrates the sign of the first saw tooth shaped carrier signal which results in a pure triangular shaped second carrier overlapped by the reference signal. The PWM signal to the power stage is made from the second carrier signal fed into a hysteresis window. The modulator loop has maintained a 1st order behavior at high frequencies, since the first comparator effectively differentiates the high frequencies, and followed by the second integrator, the -90º phase shift at high frequencies is maintained. The variable modulator forward gain is made by the second carrier signal, which will be a triangular shaped signal overlapped by the reference signal corresponds to the gain of the second integrator, which means that the switching frequency will have larger deviations from a constant value with high frequency reference signals at high levels, but if the time.

IX. SIMULINK DIAGRAM

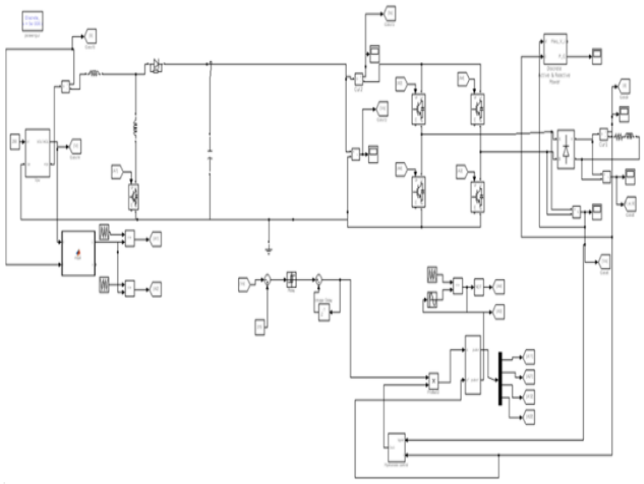

Fig.11.simulink diagram

The variable hysteresis window is made such that it follows the square of the absolute value as well as the derivative of the input signal, the switching frequency can be made constant, but at a much higher system complexity than the basic design. In this paper a second integrator block inserted before the hysteresis window in either a current or a voltage mode controller is proposed to obtain a close to constant switching frequency, regardless of M. The extraintegrator integrates the sign of the first saw tooth shaped carrier signal which results in a pure triangular shaped second carrier overlapped by the reference signal. The PWM signal to the power stage is made from the second carrier signal fed into a hysteresis window. The modulator loop has maintained a 1st order behavior at high frequencies, since the first comparator effectively differentiates the high frequencies, and followed by the second integrator, the -90º phase shift at high frequencies is maintained.

The variable modulator forward gain is made by the second carrier signal, which will be a triangular shaped signal overlapped by the reference signal. For a DC reference signal, the second integrator will simply increase the forward gain by shift the second carrier signal with respect to ground, and ideally obtaining exactly the same forward gain and thereby the same switching frequency at all modulation indexes,

ISSN(Online) : 2319 - 8753
ISSN (Print) : 2347 - 6710

International Journal of Innovative Research in Science, Engineering and Technology

(An ISO 3297: 2007 Certified Organization)

Vol. 4, Special Issue 6, May 2015

X. SIMULINK RESULT

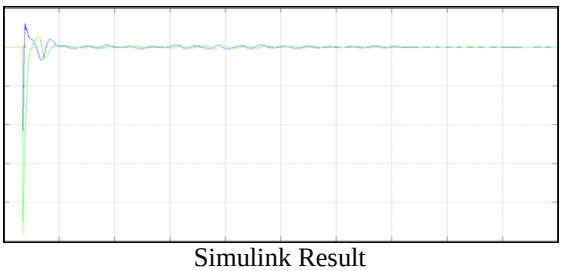

Simulink Result

XI. CONCLUSION

This paper proposed a SRPC method along with the CASDM for the single-phase grid-connected PV inverter with RPC.The proposed SRPC method can reduce the computational burden of the processor significantly, so a low-cost MCU can be adopted to implement the cost-effective PV inverter. Also, the small signal analysis for the CASDM is presented to prove the control stability. With both the SRPC and CASDM, the single-phase PV inverter can achieve the desired RPC with low current harmonic distortion. Different experimental waveforms are presented to verify the performance of the prototype circuit.

REFERENCES

[1] H. Kanchev, D. Lu, F. Colas, V. Lazarov, and B. Francois, "Energy management and operational planning of a microgrid with a PV-based activegenerator for smart grid applications," IEEE Trans. Ind. Electron., vol. 58,no. 10, pp. 4583–4592, Oct. 2011.
[2] C. Liu, P. Sun, J.-S. Lai, Y. Ji, M. Wang, C.-L. Chen, and G. Cai, "Cascade dual-boost/buck active-front-end converter for intelligent universal transformer," IEEE Trans. Ind. Electron., vol. 59, no. 12, pp. 4671–4680,Dec. 2012.
[3] C.Nagarajan and M.Madheswaran - 'Performance Analysis of LCL-T Resonant Converter with Fuzzy/PID Using State Space Analysis"- Springer, Electrical Engineering, Vol.93,March 2011.
[4] C.Nagarajan and M.Madheswaran, Stability Analysis of Series Parallel Resonant Converter with Fuzzy Logic Controller Using State Space Techniques", Taylor & Francis, Electric Power Components and Systems, Vol.39 (8), pp.780-793, 2011.
[5] C.Nagarajan and M.Madheswaran - 'Experimental verification and stability state space analysis of CLL-T Series Parallel Resonant Converter' - Journal of ELECTRICAL ENGINEERING, Vol.63 (6), pp.365-372, Dec.2012.
[6] C.Nagarajan and M.Madheswaran – 'Analysis and Implementation of LLC-T Series Parallel Resonant Converter with Fuzzy controller'- International Journal of Engineering Science and Technology (IJEST), Applied Power Electronics and Intelligent Motion Control. Vol.2 (10), pp 35-43, December 2010
[7] C.Nagarajan and M.Madheswaran - 'Performance Estimation of LCL-T Resonant Converter with Fuzzy / PID Controller'- International Journal of Computer and Electronic Engineering (IJCEE), Vol.2 (3), pp.534-542, June 2010
[8] C. Nagarajan, M.Madheswaran and D.Ramasubramanian- 'Development of DSP based Robust Control Method for General Resonant Converter Topologies using Transfer Function Model'- Acta Electrotechnica et Informatica Journal , Vol.13 (2), pp.18-31,April-June.2013
[9] C.Nagarajan and M.Madheswaran - 'DSP Based Fuzzy Controller for Series Parallel Resonant converter'- Springer, Frontiers of Electrical and Electronic Engineering, Vol. 7(4), pp. 438-446, Dec.12.
[10] C.Nagarajan and M.Madheswaran - 'Experimental Study and steady state stability analysis of CLL-T Series Parallel Resonant Converter with Fuzzy controller using State Space Analysis'- Iranian Journal of Electrical & Electronic Engineering, Vol.8 (3), pp.259-267, September 2012.
[11] H. J. Avelar, W. A. Parreira, J. B. Vieira, L. C. G. de Freitas, and E. A. A. Coelho, "A state equation model of a single-phase grid-connected inverter using a droop control scheme with extra phase shift control action," IEEE Trans. Ind. Electron., vol. 59, no. 3, pp. 1527–1537, Mar. 2012.
[12] X. Li and A. K. S. Bhat, "A utility-interfaced phase-modulated high frequency
[13] isolated dual LCL dc/ac converter," IEEE Trans. Ind. Electron., vol. 59, no. 2, pp. 1008–1019, Feb. 2012.
[14] W. Sinsukthavorn, E. Ortjohann, A. Mohd, N. Hamsic, and D. Morton, "Control strategy for three-/four-wire-inverter-based distributed generation," IEEE Trans. Ind. Electron., vol. 59, no. 10, pp. 3890–3899, Oct. 2012.
[15] J. Liu, J. Yang, and Z. Wang, "A new approach for single-phase harmonic current detecting and its application in a hybrid active power filter," in Proc. IEEE IECON/IECON, 1999, pp. 849–854.
[16] Q. Zhang, X.-D. Sun, Y.-R. Zhong, M. Matsui, and B.-Y. Ren, "Analysis and design of a digital phase-locked loop for single-phase grid-connected power conversion systems," IEEE Trans. Ind. Electron., vol. 58, no. 8, pp. 3581–3592, Aug. 2011.